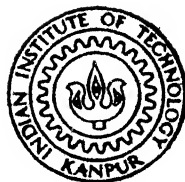


AN EXPERIMENTAL INVESTIGATION OF DAMPING CAPACITY  
OF  
SOME VISCOELASTIC MATERIALS

by  
D. V. GIRISH

ME 7h  
1979 ME/1979/m  
M GU43e  
GIR  
DNV



DEPARTMENT OF MECHANICAL ENGINEERING  
INDIAN INSTITUTE OF TECHNOLOGY, KANPUR

September 1979

**AN EXPERIMENTAL INVESTIGATION OF DAMPING CAPACITY  
OF  
SOME VISCOELASTIC MATERIALS**

A Thesis Submitted  
In Partial Fulfilment of the Requirements  
for the Degree of  
MASTER OF TECHNOLOGY

by  
D. V. GIRISH

to the  
DEPARTMENT OF MECHANICAL ENGINEERING  
INDIAN INSTITUTE OF TECHNOLOGY, KANPUR

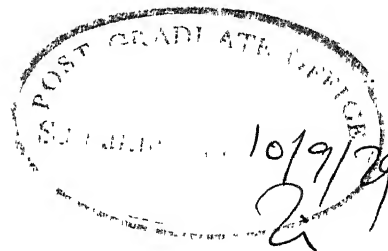
September 1979

U.S. DEPARTMENT OF  
CENTRAL INTELLIGENCE

Doc No. A 62210

7 MAY 1980

ME-1979-M-GIR-ENV



## CERTIFICATE

This is to certify that the thesis entitled  
"An Experimental Investigation of Damping Capacity of  
Some Viscoelastic Materials" by D.V. Girish is a record  
of work carried out under my supervision and has not been  
submitted elsewhere for a degree.

A handwritten signature in cursive script, appearing to read "A.K. Mallik".

A.K. Mallik  
Assistant Professor  
Department of Mechanical Engineering  
Indian Institute of Technology  
Kanpur

September 1979

RECEIVED  
for the  
Master  
in  
the  
of  
the  
of  
20.9.79 21

## ACKNOWLEDGEMENT

The author expresses his heartfelt gratitude and sincere thanks to Dr. A.K. Mallik for giving invaluable guidance and encouragement during the course of this work.

The author would like to thank Mr. M.M. Singh for rendering his services whenever needed. He is also thankful to all the staff members of Mechanical Engineering Laboratories.

Thanks are due to all his friends for their timely help.

Finally, he thanks Mr. J.C. Varma and Mr. Ram Sahai Dubey for tracings and Mr. J.D. Varma for typing of the manuscript.

## CONTENTS

	Page
CERTIFICATE	ii
ACKNOWLEDGEMENT	iii
LIST OF FIGURES	vi
LIST OF TABLES	vii
SYNOPSIS	viii
CHAPTER 1 INTRODUCTION	1
1.1 Introduction	1
1.2 Short Review of Previous Work	2
1.3 Objective and Scope of the Present Work	5
CHAPTER 2 REVIEW OF DAMPING NOMENCLATURE AND TREATMENTS	7
2.1 Damping Nomenclature for Viscoelastic Materials	7
2.2 Theory of Unconstrained Layer Damping Treatment	9
CHAPTER 3 EXPERIMENTAL SET-UP AND METHOD OF MEASUREMENTS	15
3.1 Test Rig	15
3.2 Principle of Excitation and Response Measurements	17
3.3 Calibration of Driving and the Pick-up Coils	19
3.4 Instrumentation and Method of Measurements	21
3.5 Chemical Analysis of Viscoelastic Materials	25
3.6 Details of Specimens	27

CHAPTER 4	RESULTS AND DISCUSSIONS	29
4.1	Materials Tested	29
4.2	Static Stiffness of the Specimens	34
4.3	Calibration of Coils	36
4.4	Specimen Loss Factor	36
4.5	Variation of Loss Factor with Frequency	39
4.6	Variation of Loss Factor with Carbon Content	41
CHAPTER 5	CONCLUSIONS	43
REFERENCES		44

## LIST OF FIGURES

FIGURE		PAGE
2.1	Dimensions Used in Analysis of a Two Layer Beam in Flexural Vibration	10
2.2	Element of a Two Layer Beam in Flexural Vibration	10
3.1	Experimental Set-Up	16
3.2	Schematic Diagram Showing the Principle of Excitation and Measurement	18
3.3	Block Diagram of the Instrumentation	22
4.1	Variation of Stress with Percentage Elongation	31
4.2	Variation of Stress with Percentage Elongation	32
4.3	Variation of Deflection with Load	35
4.4	Calibration Curves for Coils	37
4.5	Variation of Specimen Loss Factor with Amplitude of Oscillation	38
4.6	Variation of Loss Factor with Frequency	40
4.7	Variation of Loss Factor with Carbon Percentage	42



## LIST OF TABLES

TABLE		PAGE
3.1	Physical Characteristics of the Aluminium Beam Used as the Base Layer	28
4.1	Chemical Compositions of Viscoelastic Materials	30
4.2	Mechanical Properties of Viscoelastic Materials	33

## SYNOPSIS

### AN EXPERIMENTAL INVESTIGATION OF DAMPING CAPACITY OF SOME VISCOELASTIC MATERIALS

A Thesis Submitted  
In Partial Fulfilment of the Requirements  
for the Degree of  
MASTER OF TECHNOLOGY

by

D.V. GIRISH

to the

Department of Mechanical Engineering  
Indian Institute of Technology, Kanpur  
September 1979

This thesis presents an experimental investigation of damping capacity of viscoelastic materials. The damping capacity has been expressed in terms of the loss factor of the material. The material loss factor is computed from the specimen loss factor of a two layer beam. The viscoelastic material has been used as an unconstrained layer on a base layer of aluminium.

Three commercial rubbers and a coir material (commercial name 'Durafoam') have been tested. A range of frequency up to 85 Hz has been covered. All measurements are taken at room temperature.

Chemical compositions of the rubbers and other mechanical properties of all the materials are also reported. An attempt has been made to correlate the damping capacity with these.

## CHAPTER 1

### INTRODUCTION

#### 1.1 Introduction

Rubber like materials, commonly known as polymers, are extensively used in the field of vibration control. For example, these are used as one of the main elements of vibration isolators. Recently these materials are increasingly being used as damping layers, both constrained and unconstrained, for plate or panel type structures. It is well known that the damping of a system is the most important parameter for controlling its resonant oscillation. The possibility of achieving "tailor made" damping properties for rubber like materials makes them most useful for controlling resonant vibration.

These polymeric materials have very long chain molecules. They derive their damping capacity mainly from the viscosity at the molecular boundaries. Their dynamic behaviours have quite well been explained by mathematical models consisting of a number of ideal springs and viscous dash pots in various combinations [1]\*. In fact this gives rise to the name 'Viscoelastic'. These models predict so called 'relaxation peaks' in their damping capacities which are also observed in practice.

---

\* Number in box brackets designate References at the end of the text.

These relaxation peaks are found by varying either the frequency of oscillation or the temperature of the material. Thus the damping property of these materials is found to be very strongly dependent (sharp peaks) on frequency and temperature. In fact, in general the damping properties of such materials are expressed as a function of "reduced frequency" to take care of both temperature and frequency variations [2].

The temperatures and frequencies at which the relaxation peaks occur can be controlled by controlling the type and amount of different additives. This fact leads to the possibility of developing synthetic rubbers having "tailor made" damping properties, i.e., having very high damping at temperature and frequency ranges of actual operation.

The existence of these sharp peaks in the curve of damping versus frequency also makes it imperative to know the nature of variation of damping before the selection of the material for a specific application.

## 1.2 Short Review of Previous Work

Research on damping properties of solid materials and their engineering significance was started almost 200 years ago. In 1784, Coulomb in his 'Memoir on Torsion' speculated on the microstructural mechanisms of damping

and recognised that the mechanisms operative at low stresses may be different from those at high stresses. He also described experiments which proved that the damping under torsional oscillations is caused by internal losses in the material. Only about fifty years ago investigations were initiated on the possible relationships between internal damping and other properties such as fatigue strength. Kimball and Lovel [3] were the first to use the property of damping for engineering applications. A brief discussion on past research work on the measurement of damping properties of viscoelastic materials is presented below.

Jones and Parin [4] proposed a method of measuring the complex modulus of viscoelastic materials when these are available only in the form of thin layers. Actually this method involves measurement of the response of a simple beam with several layers of the damping tape attached to the entire surface and comparing the results with prior tests on the same configuration with another viscoelastic material having known properties. To have satisfactory results by this technique, it is absolutely necessary to obtain the initial data on the standard material. A special set up was used and the input acceleration was controlled at the shaker table and the output acceleration was measured over a range of resonant frequencies. The loss factor  $\eta$ , of the viscoelastic material was readily derived from the

measured input acceleration  $\ddot{X}$  and the output acceleration  $\ddot{Y}$ . The loss factor  $\eta$  is given by

$$\eta = (A^2 - 1)^{-1/2}$$

where

$$A = |\dot{Y} / \dot{X}| \text{ at resonance.}$$

R. De. Marie [ 5 ] developed a test rig for measurement of the damping capacity of rubber like materials loaded in compression and concluded that the energy dissipated at unit stress amplitude at relatively low frequencies - (40 Hz to 120 Hz) is usually much larger than that at higher frequencies. This was attributed to the very high rate of deformation at higher frequencies. Several damping mechanisms, like thermo-elastic mechanism, have been found to contribute significantly only at lower frequencies.

M. Horio and S. Onogi [ 6 ] described a very satisfactory method for the measurements of viscoelastic properties of materials. They used a vibrating reed in which the displacement of the free end was measured with changing the frequency of excitation applied at the clamped end of the reed. The resonant frequency and the band width of the frequency response curves were used to compute the dynamic Young's modulus of the materials. In this work a frequency range of 10 - 500 Hz was covered.

Recently, a number of machines have been developed [7] to measure the two components of the complex modulus, namely the elastic modulus and the loss modulus of visco-elastic materials. This is usually done by direct measurement of the ratio of the applied stress to the quadrature and the in-phase components of the resulting strain. The loss modulus is also determined by measuring the area of mechanical hysteresis loop, that is, the stress-strain or the force-deflection curve during cyclic loading.

### 1.3 Objective and Scope of the Present Work

The major objective of the present work is to measure the damping capacity of various rubber like materials at different frequencies. The major difficulties of measuring the damping capacity of these materials include

- i) making suitable specimens,
- ii) inherent high damping of the material.

In the present work the damping capacity of the material is expressed in terms of its loss factor. Loss factor of materials are usually calculated from that of the specimen. Usual methods of measurement of damping like, logarithmic decrement of free vibration, band width of frequency response curve, etc., have an inherent assumption of small damping. This will be violated for such materials even if it is possible to make suitable specimens.



In this work the polymeric material has been first applied as an unconstrained layer on an aluminium beam specimen. Then the overall loss factor of the composite specimen has been measured. Thereafter, the loss factor of the material has been computed. This computation has been based on well developed theory [ 8 ] , reviewed briefly in Section 2.2., with the assumption that the damping capacity of the base layer is negligible.

The method of determination of the loss factor of the composite specimen is based on the measurement of energy input to maintain a steady state harmonic resonant oscillation [ 9 ] . The experimental set-up developed in reference [ 9 ] has been used.

Four different materials have been tested in the present work and a frequency range of 10 - 85 Hz has only been covered. At a particular frequency, the data has been averaged over three different thickness ratios of the damping layer and the basic material.. Readings have been taken at various amplitudes of oscillation and the damping, as expected, has been found to be independent of this amplitude. Correction for air damping has been found to be insignificant.

Static mechanical properties and chemical compositions of the materials have also been obtained. Attempts have been made to correlate these with the nature of change in the damping capacity. All the readings have been taken at room temperature.

## CHAPTER 2

### REVIEW OF DAMPING NOMENCLATURE AND TREATMENTS

#### 2.1 Damping Nomenclature for Viscoelastic Materials

The dynamic stress strain relationship for a viscoelastic material is not governed by a simple proportionality rule [1]

Let the harmonic applied stress be

$$\sigma = \sigma_o e^{j\omega t} \quad (2.1)$$

when the resulting strain for such materials can be expressed as

$$\epsilon = \epsilon_o e^{j\omega t} \quad (2.2)$$

where  $\omega$  = frequency.

It is seen that the ratio

$$\begin{aligned} \frac{\sigma}{\epsilon} &= \frac{\sigma_o}{\epsilon_o} \text{ is a complex quantity} \\ &= a + j b \text{ ( say )} \end{aligned} \quad (2.3)$$

In general both 'a' and 'b' are found to be frequency and temperature dependent.

$$\text{Thus, } a = a(\omega, \theta)$$

$$\text{and } b = b(\omega, \theta)$$

where  $\theta$  denotes the temperature.

The ratio of the stress and the strain as given by Equation (2.3) is called as the dynamic (complex) modulus of the material.

$$\begin{aligned} E^* (\omega, \theta) &= a (\omega, \theta) + j b (\omega, \theta) \\ &= E_r (\omega, \theta) + j E_i (\omega, \theta) \end{aligned} \quad (2.4)$$

where the real part  $E_r$ , is called the storage modulus and the imaginary part  $E_i$ , is termed as the loss modulus. The storage modulus signifies the component of the strain which is in phase with the applied stress. The loss modulus, on the other hand, signifies the component of the strain which is in quadrature with the applied stress. The ratio of loss modulus and the storage modulus is termed as the loss factor  $\eta$ , thus

$$\eta (\omega, \theta) = \frac{E_i (\omega, \theta)}{E_r (\omega, \theta)} \quad (2.5)$$

So the complex modulus can be written as

$$E^* (\omega, \theta) = E_r (\omega, \theta) [1 + j \eta (\omega, \theta)]$$

The non-dimensional ratio, known as loss factor and given by equation (2.5) can easily be shown equal to

$$\eta = \frac{D}{2\pi U} \quad (2.6)$$

where

$D$  = energy dissipated per unit volume per cycle by the material,

and  $U$  = maximum elastic energy stored by unit volume of the material in that cycle.

The quantity  $\eta$  is the most common expression for the damping capacity of linear viscoelastic materials. It should be noted that all relations from equations (2.1) to (2.6) (and hence the loss factor definition) presupposes harmonic motion. This index of damping can be easily related to other commonly used measures of damping capacity.

In the present work the variation  $E_r$  with frequency has been neglected as it is usually rather small except at very high frequencies or low temperatures when rubber to glass transition takes place.

## 2.2 Theory of Unconstrained Layer Damping Treatment

The expression for the overall loss factor of a composite beam consisting of a non dissipative base layer with an unconstrained viscoelastic layer at the top is derived in this section. The analysis follows the generalized approach for a three layer beam presented by Kerwin, Ross, and Ungar [8].

Figure 2.1 shows a composite beam, made of an elastic base layer with a viscoelastic layer at the top. The neutral plane of the composite beam is displaced by an amount  $D$ , from the centre of the original beam due to the addition of a damping layer. The thickness and other distances used in the analysis are also shown in Figure (2.1).

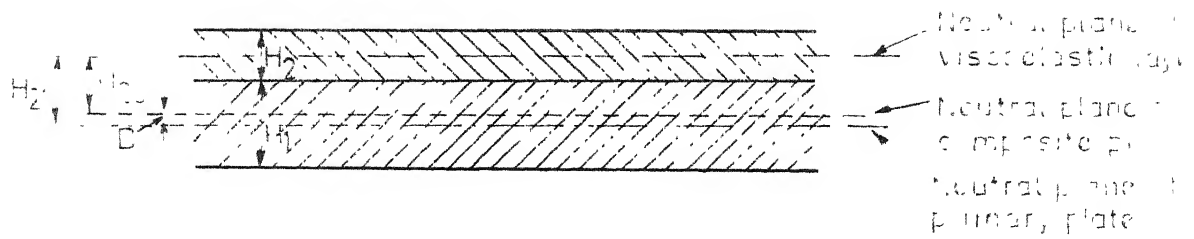


Fig.2.1 Dimensions used in analysis of a two layer beam in flexural vibration

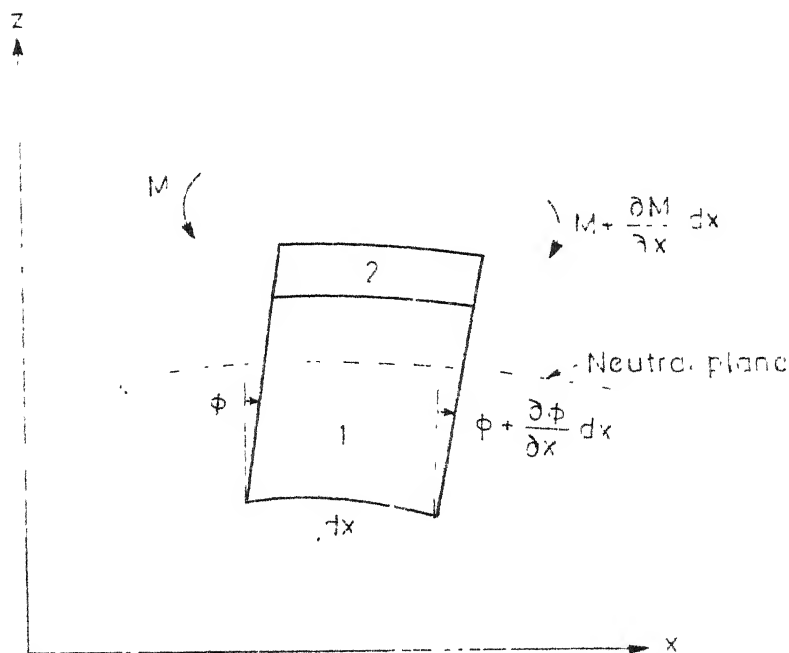


Fig.2.2 Element of a two layer beam in flexural vibration

Figure (2.2) represents an element of a two layer beam in flexure. The angle  $\phi$ , is the flexural angle of the base plate represented by layer 1, in Figure (2.1).

Now considering a unit width of the 2-layer element, one can express the total bending moment  $M$ , as

$$M = B \frac{\partial \phi}{\partial x} = \sum_{i=1}^2 M_{ii} + \sum_{i=1}^2 F_i H_{io} \quad (2.7)$$

where

- $B$  = flexural rigidity of the cross section,  
 $M_{ii}$  = the moment exerted by the forces on the  $i^{\text{th}}$  layer about its own neutral axis,  
 $F_i$  = net extensional force on the  $i^{\text{th}}$  layer, and  
 $H_{io}$  = the distance from the centre of the  $i^{\text{th}}$  layer to the neutral plane of the composite beam.

The various individual moments  $M_{ii}$  may be expressed in terms of the curvatures, as

$$\begin{aligned} M_{11} &= E_1 I_1 \frac{\partial \phi}{\partial x} \\ &= E_1 \frac{1}{12} H_1^3 \frac{\partial \phi}{\partial x} \\ &= K_1 \frac{H_1^2}{12} \frac{\partial \phi}{\partial x} \end{aligned} \quad (2.8)$$

where,  $K_1 = E_1 H_1$ , the extensional stiffness of a unit length of layer 1.

Similarly,

$$M_{22} = K_2 \frac{H_2^2}{12} \frac{\partial \phi}{\partial x} \quad (2.9)$$

where,  $K_2 = E_2 H_2$ , is the extensional stiffness of a unit length of layer 2.

The net extensional force on each layer is obtained by integrating the stresses over the layer. One can deduce that the net extensional force in a given layer is given by the product of the extensional stiffness of the layer and extensional strain at its mid-plane. Therefore,

$$\begin{aligned}
 F_1 &= \text{Extensional force in the first layer} \\
 &= E_1 A_1 \frac{\partial u_1}{\partial x} \\
 &= E_1 (H_1 \times 1) \frac{\partial}{\partial x} (H_{10} \times \phi) \\
 &= E_1 H_1 \cdot H_{10} \frac{\partial \phi}{\partial x} \\
 &= K_1 H_{10} \frac{\partial \phi}{\partial x} \quad (2.10)
 \end{aligned}$$

Similarly one can write

$$\begin{aligned}
 F_2 &= \text{Extensional force in the second layer} \\
 &= K_2 H_{20} \frac{\partial \phi}{\partial x} \quad (2.11)
 \end{aligned}$$

In pure flexure, the net extensional force on each of the composite element must vanish, that is

$\sum F_i = 0$ . Hence,

$$\sum_{i=1}^2 F_i = K_1 H_{10} \frac{\partial \phi}{\partial x} + K_2 H_{20} \frac{\partial \phi}{\partial x} = 0 \quad (2.12)$$

By expressing

$$\text{and } \left. \begin{aligned} H_{10} &= -D \\ H_{20} &= H_{21} - D \end{aligned} \right\} \quad (2.13)$$

and substituting in equation (2.12) one can write,

$$\sum_{i=1}^2 F_i = \{ -K_1 D + K_2 (H_{21} - D) \} \frac{\partial \phi}{\partial x} = 0 \quad (2.14)$$

From equation (2.14) one can express the value of  $D$ , the displacement of the neutral plane, as

$$D = \frac{K_2 H_{21}}{(K_1 + K_2)} \quad (2.15)$$

Using equations (2.8), (2.9), (2.10), (2.11) and (2.13) in equation (2.7), one can write an expression for flexural rigidity as

$$B = K_1 \frac{H_1^2}{12} + K_2 \frac{H_2^2}{12} + K_1 D^2 + K_2 D^2 + K_2 H_{21}^2 - 2 K_2 D H_{21} \quad (2.16)$$

The loss factor  $\eta_s$  of the composite beam can now be determined by replacing the appropriate elastic moduli by complex quantities and finding the real and imaginary components of the flexural rigidity.

By expressing  $K_2^* = K_2 (1 + i \eta_2)$ , and  $K_1^* = K_1$  (i.e., a non-dissipative base plate) an expression for loss factor,  $\eta_s$ , is obtained as

$$\eta_s = \frac{b''_{e_2}}{b'} \quad (2.17)$$

where  $b''_{e_2} = \eta_2 k_2 [12 h_{21}^2 + h_2^2]$

and  $b' = 1 + k_2 [12 h_{21}^2 + h_2^2]$



where the lower case symbols represent the dimensions and stiffness denoted by the upper case symbols divided by the corresponding properties of the base plate

$$[ \text{i.e., } k_2 = \frac{K_2}{K_1}, \quad h_2 = \frac{H_2}{H_1}, \quad h_{21} = \frac{H_{21}}{H_1} = \frac{H_1 + H_2}{2 H_1} ] .$$

By expressing  $h_{21}$  in terms of thicknesses of the two layers and replacing  $k_2$  by  $e_2 h_2$  one may write equation (2.17) as

$$\eta_s = \frac{\eta_2 e_2 h_2 [ 3 + 6 h_2 + 4 h_2^2 ]}{1 + e_2 h_2 [ 3 + 6 h_2 + 4 h_2^2 ]} \quad (2.18)$$

$$\text{where } e_2 = \frac{E_2}{E_1} .$$

In the present work equation (2.18) has been used for determining the loss factor of the treatment material. The value of the composite loss factor  $\eta_s$  is determined experimentally for three different values of the relative thickness of the damping layer,  $h_2 = \left( \frac{H_2}{H_1} \right)$ . The value of  $E_2$ , has also been obtained experimentally.

The values of  $\eta_2$ , the loss factor of the viscoelastic material (now onwards to be represented by  $\eta$ ) was then calculated for different values of relative thickness of damping layer under a specified frequency. Then the average of these values has been taken as the loss factor of the viscoelastic material at that frequency.

## CHAPTER 3

### EXPERIMENTAL SET-UP AND METHOD OF MEASUREMENTS

#### 3.1 Test Rig

The test rig consists mainly of a steel frame bolted rigidly to a massive concrete foundation (Figure 3.1) [9]. The composite beam specimen is clamped vertically at one end while the other end carries an aluminium inertia bar. Here the beam and the inertia bar combination has been idealised as a single degree of freedom system. Four coils are fitted symmetrically to the inertia bar as shown in Figure 3.2. Each of these coils moves in the field of four pairs of permanent bar magnets during the oscillation of the specimen. This combination of coil and magnet system can be used as excitation or pick up units. Magnets are held on position within aluminium magnetic holders. The aluminium magnetic holders are in turn secured firmly to the main steel frame. The gap between the pair of magnets is adjustable so that the field strength across the coils can be varied.

A travelling microscope measures the vibration amplitude of the specimen along with the inertia bar. One side of the steel frame is provided with a window so as to permit the movement of the travelling microscope.

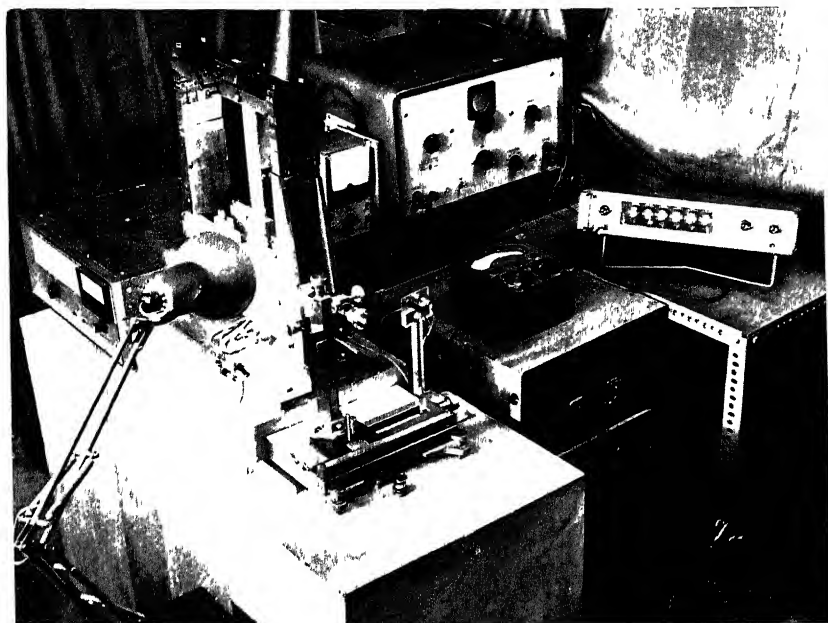


FIGURE 3.1      EXPERIMENTAL SET-UP

### 3.2 Principle of Excitation and Response Measurements

For the purpose of excitation, current from an oscillator through a power amplifier is fed in series to the **two** coils on the same side (say coil '1' and coil '2', Figure 3.2). As a result, both the coils are subjected to forces of magnitudes say  $F_1$  and  $F_2$ , as shown in Figure 3.2. Thus the combination of the beam and inertia bar is subjected to a resultant force  $F_1 + F_2$ . With the negligible difference between  $F_1$  and  $F_2$ , the beam is subjected primarily to bending mode of oscillation. This is ensured further by varying the frequency of the supply current so as to resonate the beam in its flexural mode.

When the beam oscillates, some voltage is generated across the other coils (coil '3' and coil '4'). This generated voltage is proportional to the velocity of oscillation. Thus these coils can be used as pick-up coils, that is for the measurement of response.

It is obvious that by using the pair of coils which are diagonally opposite (say coil '2' and coil '3') as the exciting coils, torsional modes of oscillations can also be generated. Similarly, using three coils simultaneously as input coils, the specimen can be subjected to combined bending and torsional oscillations.

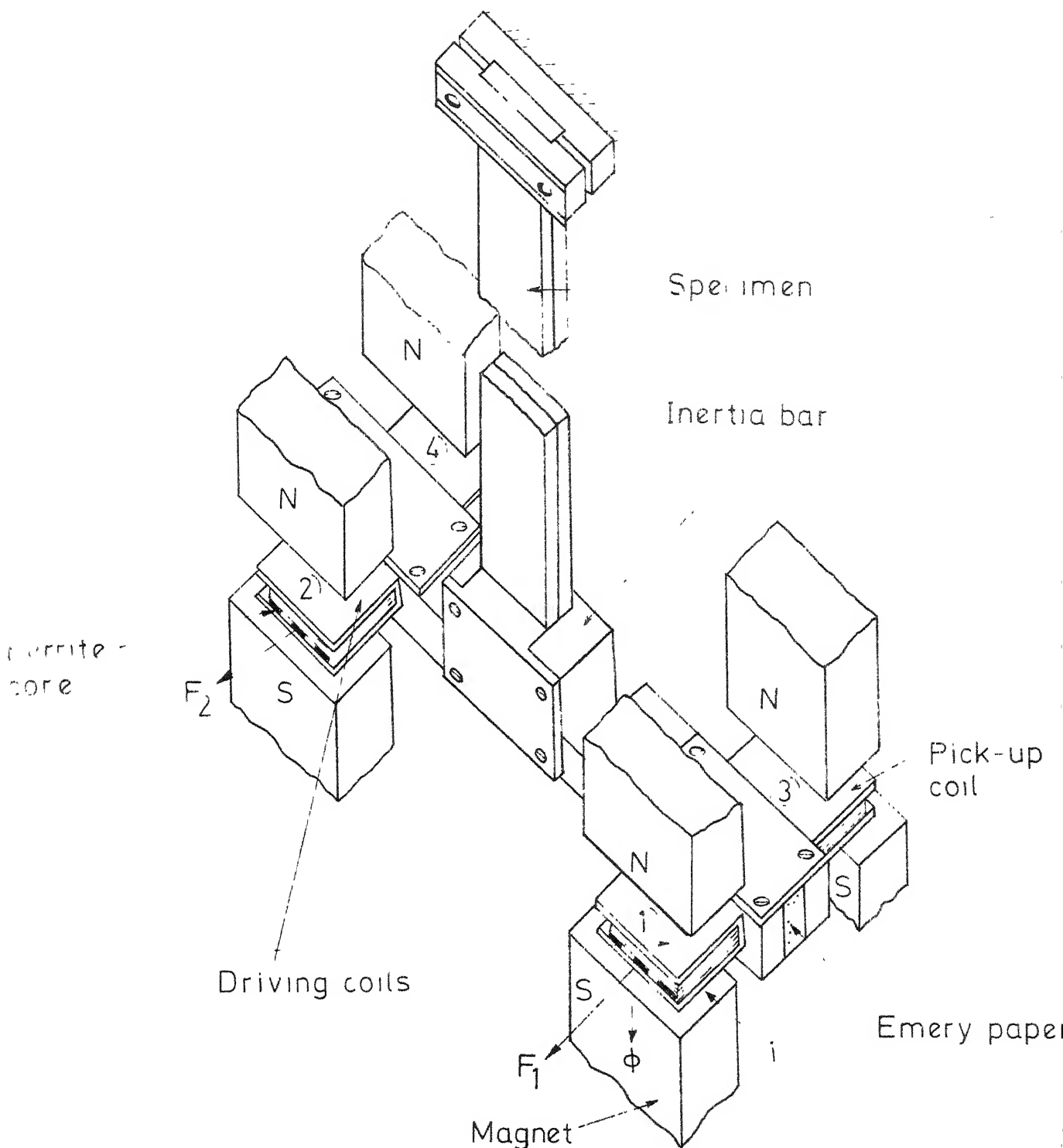


Fig.32 Schematic diagram showing the principle of excitation and measurement

### 3.3 Calibration of the Driving and the Pick-up Coils

As stated earlier, the specimen is excited by sinusoidal force at resonance. The driving coils are fed with alternating current of known frequency and amplitude after amplification. The exciting force generated by the driving coil (say coil 'j')  $F_j$  is given by

$$F_j = B_j l_j i_j \quad \text{Newtons} \quad (3.1)$$

where

$B_j$  = magnetic inductance (Webers/  $m^2$ )

$l_j$  = length of current carrying conductor (metre)

$i_j$  = current passing through the driving coils  
(ampere).

Thus the force amplitude of the  $j^{\text{th}}$  coil,

$$\begin{aligned} F_j &= \sqrt{2} B_j l_j (i_j)_{\text{rms}} \\ &= 2 \frac{B_j l_j}{\sqrt{2}} (i_j)_{\text{rms}} \\ &= 2 r_j (i_j)_{\text{rms}} \end{aligned} \quad (3.2)$$

where  $r_j = \frac{(B l)_j}{\sqrt{2}}$ , is called the calibration factor for the driving coil, (as explained later). (3.3)

The output voltage generated in the measuring coil moving with a velocity  $v$ , is given by

$$V_p = B_p l_p v \quad \text{volts} \quad (3.4)$$

$$\text{Or, } \sqrt{2} (V_p)_{\text{rms}} = B_p l_p v_{\text{amplitude}}$$

$$\begin{aligned} \text{Hence } (V_p)_{\text{rms}} &= B_p l_p \frac{v_{\text{amplitude}}}{\sqrt{2}} \\ &= r_p v_{\text{amplitude}} \end{aligned} \quad (3.5)$$

$$\text{where } r_p = \frac{B_p l_p}{\sqrt{2}} \quad (3.6)$$

is called ~~the~~ calibration factor for the pick-up coil.

If  $x$  = amplitude of vibration  
then the amplitude of velocity of oscillation of the inertia bar

$$\begin{aligned} v_{\text{amplitude}} &= \omega x \\ &= 2\pi f_n x \\ &= \pi f_n X_{pp} \end{aligned} \quad (3.7)$$

where  $f_n$  = frequency of oscillation (Hz) and

$X_{pp}$  = peak-to-peak displacement of the coil.

It can be seen from equations (3.3) and (3.6) that if a coil is calibrated as a pick-up coil, it is simultaneously calibrated as a driving coil also. Therefore, by measuring the different values of  $(V_p)_{\text{rms}}$ ,  $X_{pp}$  and  $f_n$ , and by using equations (3.5) and (3.7), all the coils can be calibrated as pick-up coils.

### 3.4 Instrumentation and Method of Measurements

Figure 3.3 shows the block diagram of the instrumentation used in the present work. The driving coils are fed from an oscillator through a power amplifier. The frequency and the rms. value of the current are measured with the help of a frequency counter and an avometer respectively. The rms. voltage generated across the pick-up coil is measured by using a milli-voltmeter. The frequency of the current is varied so as to maximise the output voltage for a given value of the current. Thus the system is vibrated at resonance. A shining sand point on the piece of fine emery paper pasted on one side of the inertia bar (shown in Figure 3.2) is viewed through a travelling microscope. As the inertia bar (composite beam) vibrates, this point when viewed through the microscope appears as a single shining line. The length of the line measured by the microscope represents the value of the peak-to-peak displacement of the coil. The least count of the vernier is 0.01 mm.

At steady state, the energy dissipated per cycle by the whole specimen under harmonic load is given by

$$D_s = \pi F_o X_o \sin \psi_o \quad (3.8)$$

where

$$\begin{aligned} D_s &= \text{energy dissipated (Joule/cycle)} \\ F_o &= \text{amplitude of exciting force (Newtons)} \\ X_o &= \text{amplitude of vibration of inertia bar} \\ &= \frac{X_{pp}}{2} \text{ (metres)} \end{aligned}$$

LIBRARY  
CENTRAL LIBRARY

Acc. No. A 62210



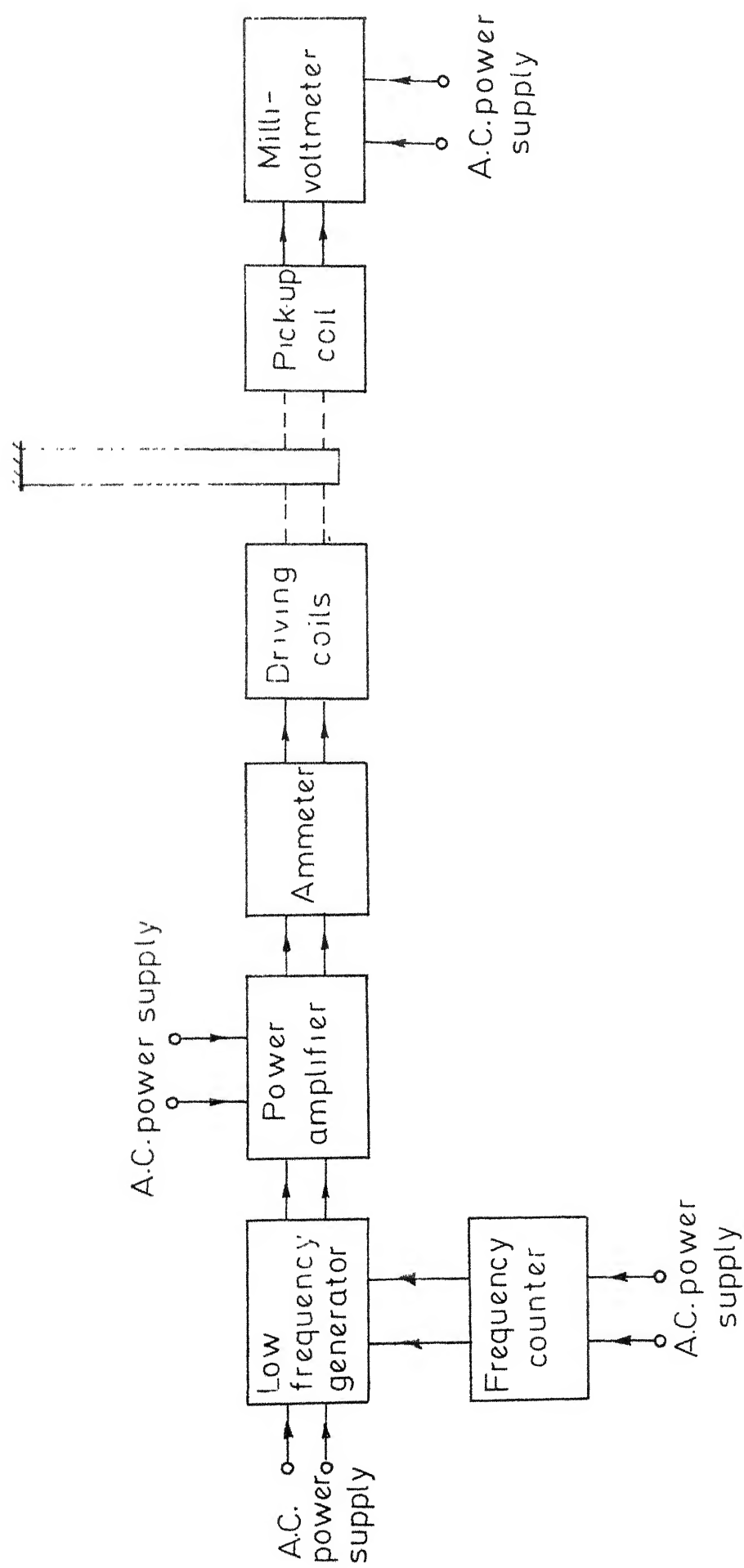


Fig.3.3 Block diagram of the instrumentation

and  $\psi_o$  = phase difference between the exciting force and the resulting displacement.

But at resonance  $\psi_o$  is approximately equal to  $90^\circ$  (for small damping).

Hence

$$D_s = \pi F_o X_o \quad (3.9)$$

Since there are two driving coils the total exciting force on the beam

$$\begin{aligned} F_o &= F_1 + F_2 \\ &= 2 (\Gamma_{d_1} + \Gamma_{d_2}) (i_j)_{rms} \end{aligned} \quad (3.10)$$

where  $\Gamma_{d_1}$  and  $\Gamma_{d_2}$  are the calibration factors for driving coils '1' and '2'.

By using equation (3.10) in equation (3.9), one can write an expression for the energy dissipated per cycle by the whole specimen,

$$D_s = 2\pi (\Gamma_{d_1} + \Gamma_{d_2}) (i_j)_{rms} X_o \quad (3.11)$$

The maximum strain energy of the system during the cycle,  $U_s$ , can be approximated as

$$\begin{aligned} U_s &= \frac{1}{2} K X_o^2 \\ &= \frac{1}{8} K X_{pp}^2 \end{aligned} \quad (3.12)$$

where  $K$  = static stiffness of the cantilever beam specimen at its free end.

The specimen loss factor  $\eta_s$ , can now be calculated from equations (3.5), (3.7), (3.11) and (3.12) as

$$\eta_s = \frac{D_s}{2 \pi U_s} = \frac{4 \pi (\Gamma_{d_1} + \Gamma_{d_2}) \Gamma_p}{K} f_n \frac{(i)_{rms}}{(V)_{rms}}$$

$$4 \pi \frac{(\Gamma_1 + \Gamma_2)}{K} \Gamma_3 f_n \frac{(i)_{rms}}{(V)_{rms}} \quad (3.13)$$

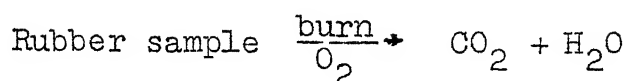
The loss factor of the material is obtained from the value of  $\eta_s$  through the use of equation (2.18) as discussed in section 2.2. This value of  $\eta$  is for the specific frequency of oscillation (first mode of the system).

To obtain the values of  $\eta_s$  (and hence of  $\eta$ ) at different frequencies, first the higher modes of the specimen and the inertia bar combination were attempted. However, it was found that even the pure second mode could not be excited. This can be attributed to the coupling of modes through damping, may be because of high damping of the system. In fact, it was found that near the second natural frequency of the system, the response was found to be the superposition of two harmonics. One of these was corresponding to the first mode and the other to the second mode. Then it was decided to use different lengths of the specimens to change their first natural frequency and always use the first mode for experimentation. With different thickness ratios and different materials, frequency of measurement was kept constant by changing the length of the specimen.

### 3.5 Chemical Analysis of Viscoelastic Materials

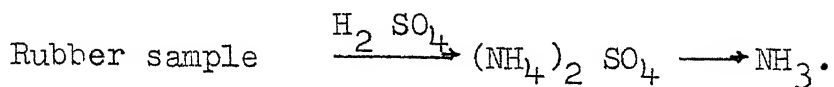
To specify the composition of the rubber materials, chemical analysis has been carried out to determine the contents of carbon, nitrogen, hydrogen, ash content etc., as discussed below [ 10 ] .

#### 3.5.1 Estimation of Carbon and Hydrogen (by Combustion process).



A definite amount of substance (Rubber pieces) is weighed using a chemical balance and kept in a small bowl placed in a combustion tube. The specimen kept in the combustion tube is heated in a stream of Oxygen in an electric furnace. However, the product is not burnt completely. The resulting products of incomplete combustion are passed through a part of the tube packed with an oxidizing filling and are heated in a furnace. The resulting products of complete combustion, water and carbon-di-oxide are absorbed in weighed tubes containing anhydrous magnesium-per-chlorate and sodalime respectively. After the absorption of water and carbon-di-oxide is completed, the magnesium-per-chlorate and sodalime are weighed again. The difference in weight of the final and the initial readings gives the weight of water and carbon-di-oxide produced and hence the percentage of carbon and hydrogen in the original compound.

### 3.5.2 Estimation of Nitrogen (Kjeldhal Method)



The rubber sample is treated with concentrated sulphuric acid according to the above chemical reaction. This reaction will yield ammonium sulphate. This ammonium sulphate is then converted into ammonia. This ammonia is then treated with any acid and thus the amount of nitrogen is determined.

### 3.5.3 Swelling

Swelling can also be used to specify a rubber. Rubber samples of known volume (say  $10 \times 10 \times 3 \text{ mm}^3$ ) are immersed in beakers containing benzene and acetone separately. The amount of swelling should be referred with respect to a specific time. Here the sample of rubber has been removed after a lapse of 24 hours and the final volume is measured to determine the percentage swelling of the rubber.

### 3.5.4 Ash Content

A known weight of rubber sample has been burnt at  $800^\circ\text{C}$  in a crucible kept in a muffle furnace. After the completion of the burning process, the crucible is taken out from the furnace and the burnt product is weighed to determine the percentage of ash content in the rubber.

### 3.6 Details of Specimens

Physical characteristics of the aluminium beam specimens used as base layer in the present work are given in Table 3.1. Various combinations of length and thickness were used to have the desired range of frequency from 10 Hz to 85 Hz. It was found that the addition of viscoelastic layer has got very little effect over the desired frequency. This little variation (if any) was corrected by adjusting the over all length of the specimen.

TABLE 3.1      Physical Characteristics of the Aluminium  
Beam Used as the Base Layer

Frequency (Hz)	9.3	18.6	40.0	60.0	81.5
Length (mm)	320.0	178.0	178.0	195.0	178.0
Thickness (mm)	3.0	3.0	6.0	9.5	12.4
Width (mm)	20.5	20.5	20.5	20.5	20.5

## CHAPTER 4

### RESULTS AND DISCUSSIONS

#### 4.1 Materials Tested

Three different rubber samples referred to as number 1, 2, and 3 respectively and a commercial Coir 'Durafoam' have been tested in the present work. The rubber compositions determined in a manner described in Section 3.5, are shown in Table 4.1.

For determination of static Young's modulus ( $E_2$ ) for these materials, standard dog-bone test samples were made from the bulk material. These were then tested in 'Instron' machine and the resulting stress-strain curves are shown in Figures 4.1 and 4.2. These figures show the values up to the breaking point. The breaking stresses and the corresponding percentage elongations are included in Table 4.2. It is clearly seen from Figures 4.1 and 4.2 that all the materials show strong non-linear behaviour. This poses a difficulty in determining the value of Young's modulus  $E_2$ , to be used in equation (2.18). It should be kept in mind that the analysis assumed a constant value for  $E_2$ . The maximum percentage elongation, the rubber layers were subjected to during oscillation of the specimens was found to be less than 0.1%. The minimum percentage elongation which can be recorded accurately in the 'Instron' machine for these specimens was found to be 0.1%. It was



Table 4.1 Chemical Compositions of Viscoelastic Materials

Viscoelastic Materials	% C	% H	% N	% Ash	Swelling	
					Benzene %	Acetone %
Rubber '1'	15.50	1.63	0.70	0.92	164	3.4
Rubber '2'	33.03	4.38	0.83	1.00	178	6.2
Rubber '3'	66.97	9.16	0.87	0.87	152	5.3

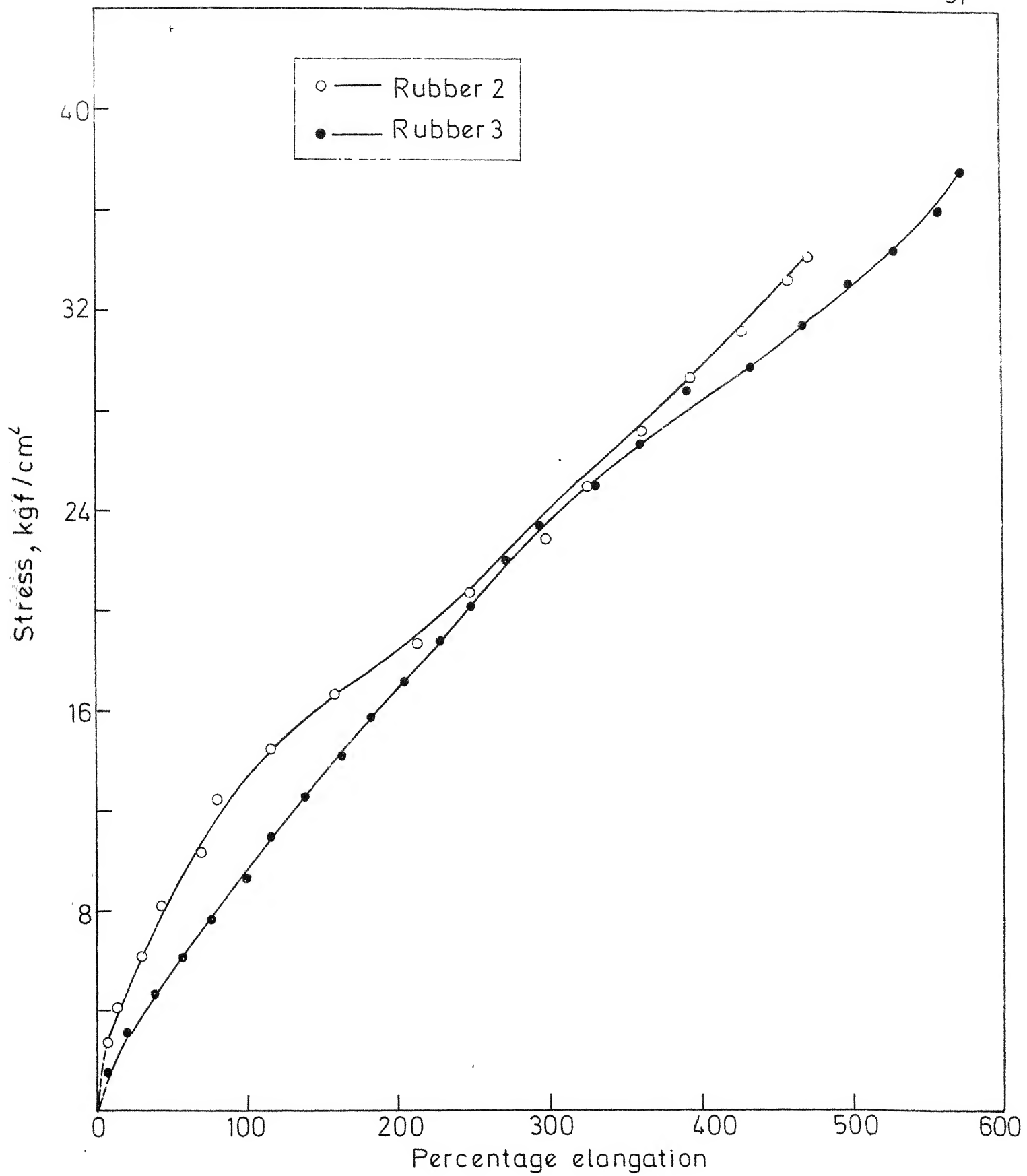


Fig.4.1 Variation of stress with percentage elongation

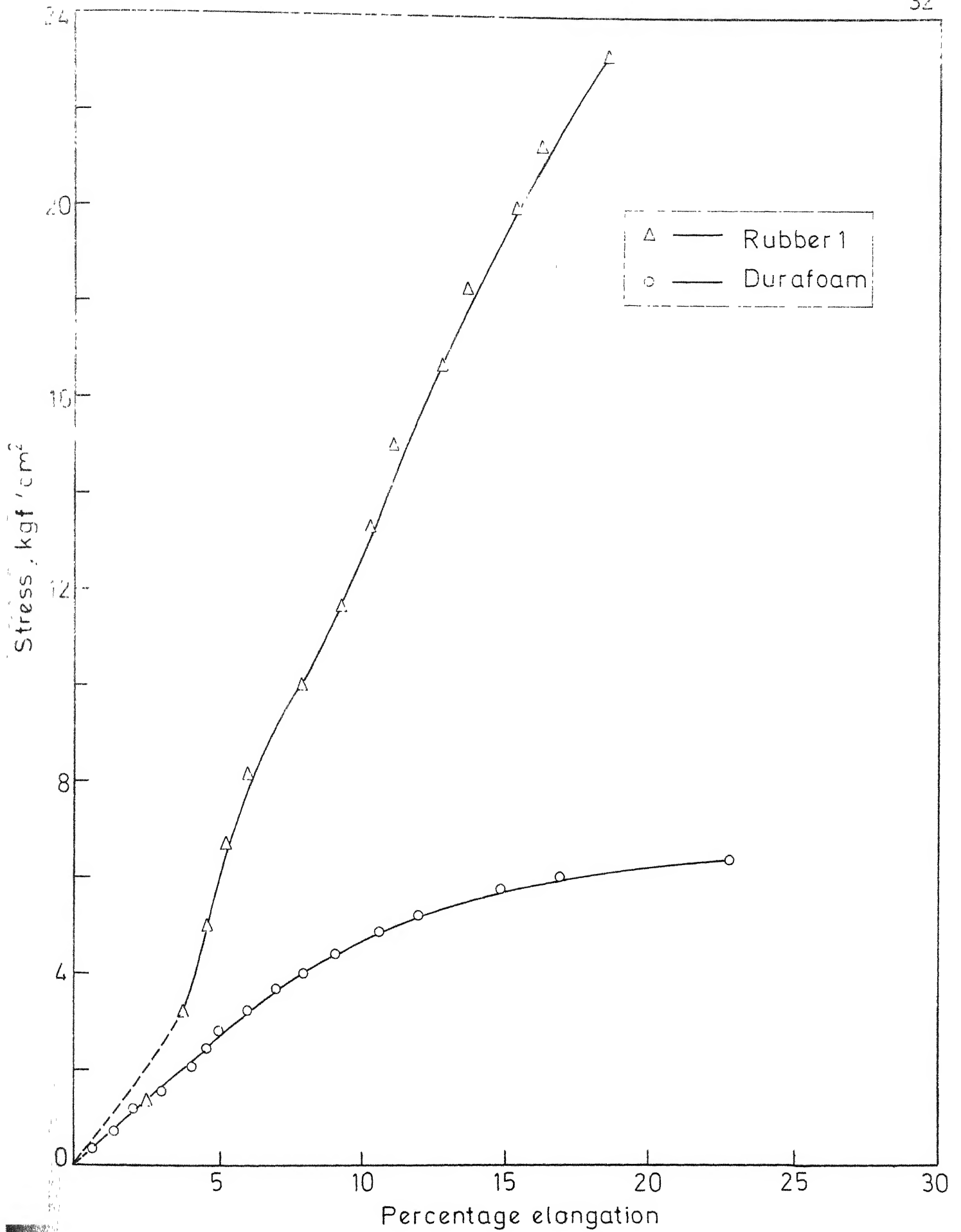


Fig 4.2 Variation of stress with percentage elongation

Table 4.2 Mechanical Properties of Viscoelastic Materials

Viscoelastic Materials	At Breaking Point		At Minimum		Percentage Elongation		Specific Gravity
	Stress Newtons/ mm <sup>2</sup>	Elongation %	Stress Newtons/ mm <sup>2</sup>	Elongation %	Young's Modulus Newtons/ mm <sup>2</sup>	E <sub>2</sub>	
Rubber '1'	2.601	21.38	0.1120	0.1	114.0		2.535
Rubber '2'	6.810	467.00	0.0760	0.1	76.84		1.684
Rubber '3'	7.512	575.00	0.0422	0.1	43.80		1.080
Durafoam	0.638	22.80	0.0214	0.1	21.93		0.630

decided then to record the applied stress levels to cause 0.1% elongation for all the specimens and the value of  $E_c$  be determined as the ratio of this stress and strain (0.001) levels. These values are also indicated in Table 4.2.

#### 4.2 Static Stiffness of the Specimens

The static stiffness of the composite beam specimens,  $K$ , to be used in equation (3.13) has been determined experimentally. This has been done by putting dead weights at the free end of the specimen, held horizontally in a clamp, and measuring the corresponding vertical deflections with the help of a travelling microscope. Figure 4.3 shows a typical load-deflection curve. The static stiffness is obtained from the slope of the straight line representing the load-deflection curve. These experimental values were also checked against the theoretical values for a cantilever given by

$$K = \frac{3 (E_1 I_1 + E_2 I_2)}{L^3}$$

where

$L$  = length of the specimen,

$E_1 I_1$  = bending rigidity of the base layer, and

$E_2 I_2$  = bending rigidity of the damping layer.

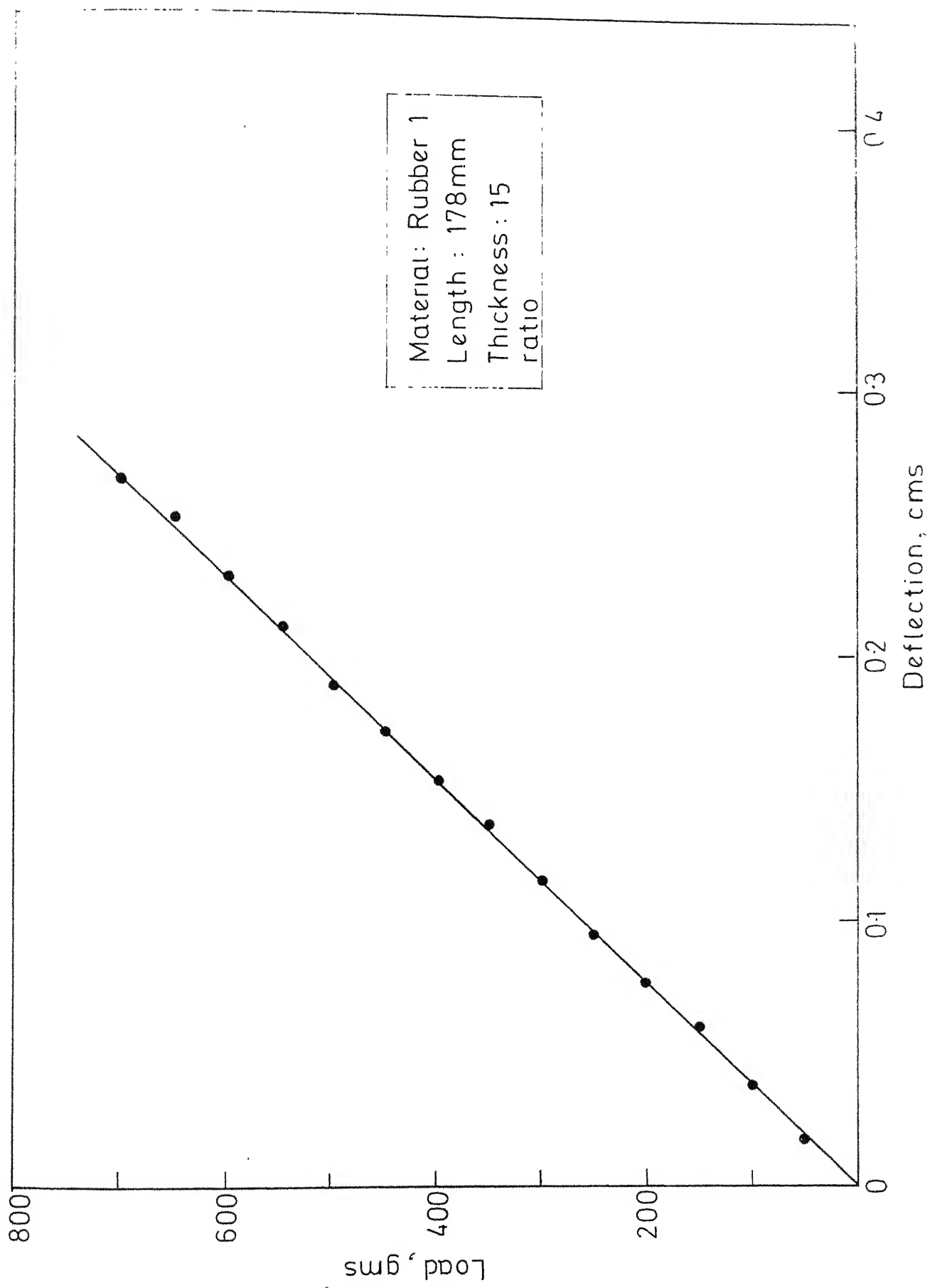


Fig.4.3 Variation of deflection with load

as  $E_2 \ll E_1$ ,  $K$  can be approximated as

$$K \approx \frac{3 E_1 I_1}{L^3}$$

The theoretical value obtained in this manner has been found to be in very good agreement with the experimental values.

### 4.3 Calibration of Coils

Typical values of the voltages generated across pick-up coils and the corresponding velocities of the inertia bar (that is, of the coil) computed from equation (3.7) are shown in Figure 4.4 for all the four coils. It can be seen that up to 32 mv, the range within which the present experiments are conducted, the voltage velocity relationship is linear. The frequency and the waveform of the voltage generated were also checked by a cathode ray oscilloscope. These calibration curves are drawn for each set of data and show little changes because of the variation of the air gap between the coil and the magnets.

### 4.4 Specimen Loss Factor

Figure 4.5 shows a typical curve of the specimen loss factor  $\eta_s$ , calculated from equation (3.13) for various values of the amplitude of oscillations. As expected for such materials, the loss factor is seen to be constant at a particular frequency. The loss factor is seen to be

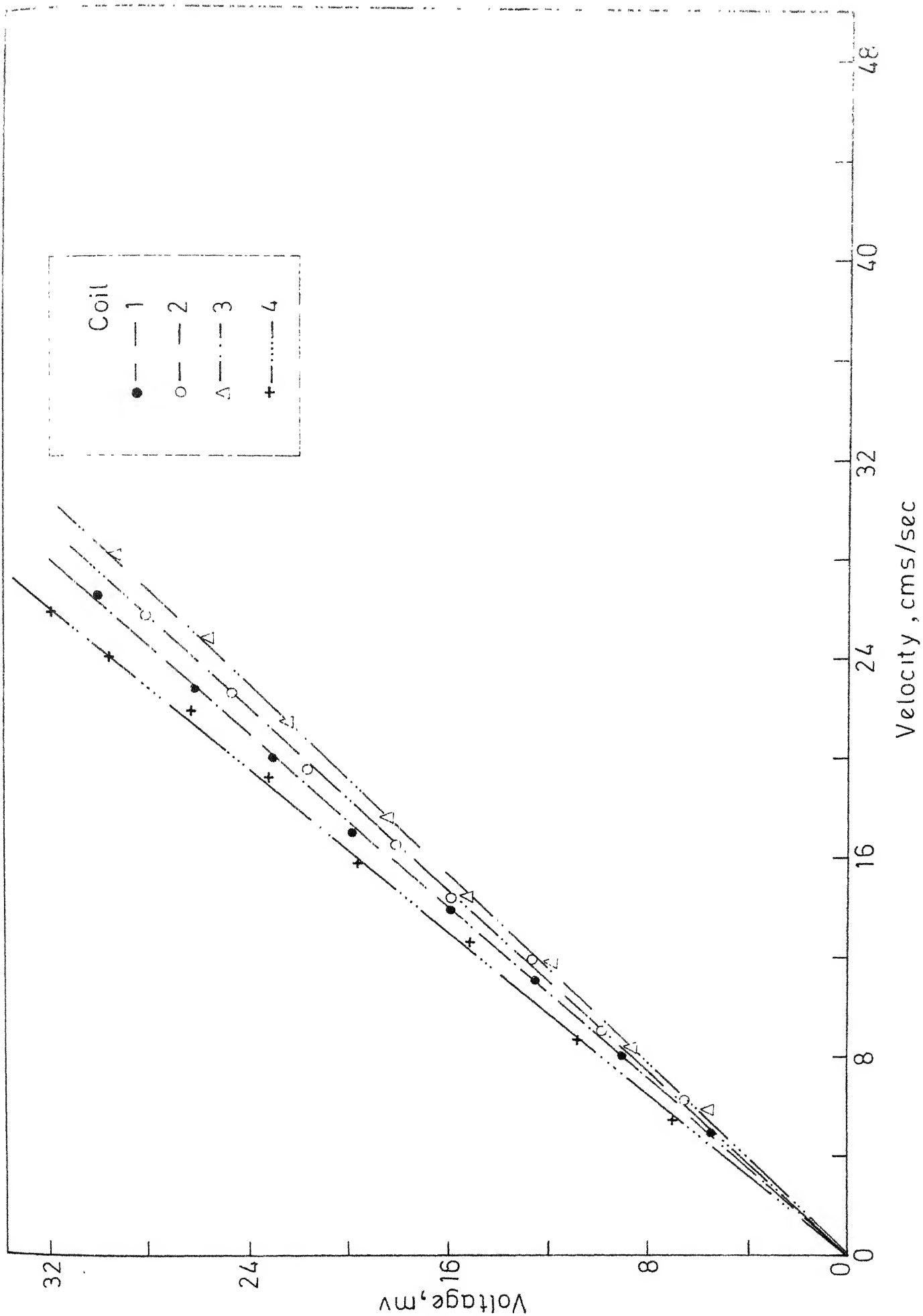


Fig. 1. Voltage vs. velocity for coils 1, 2, 3, and 4.



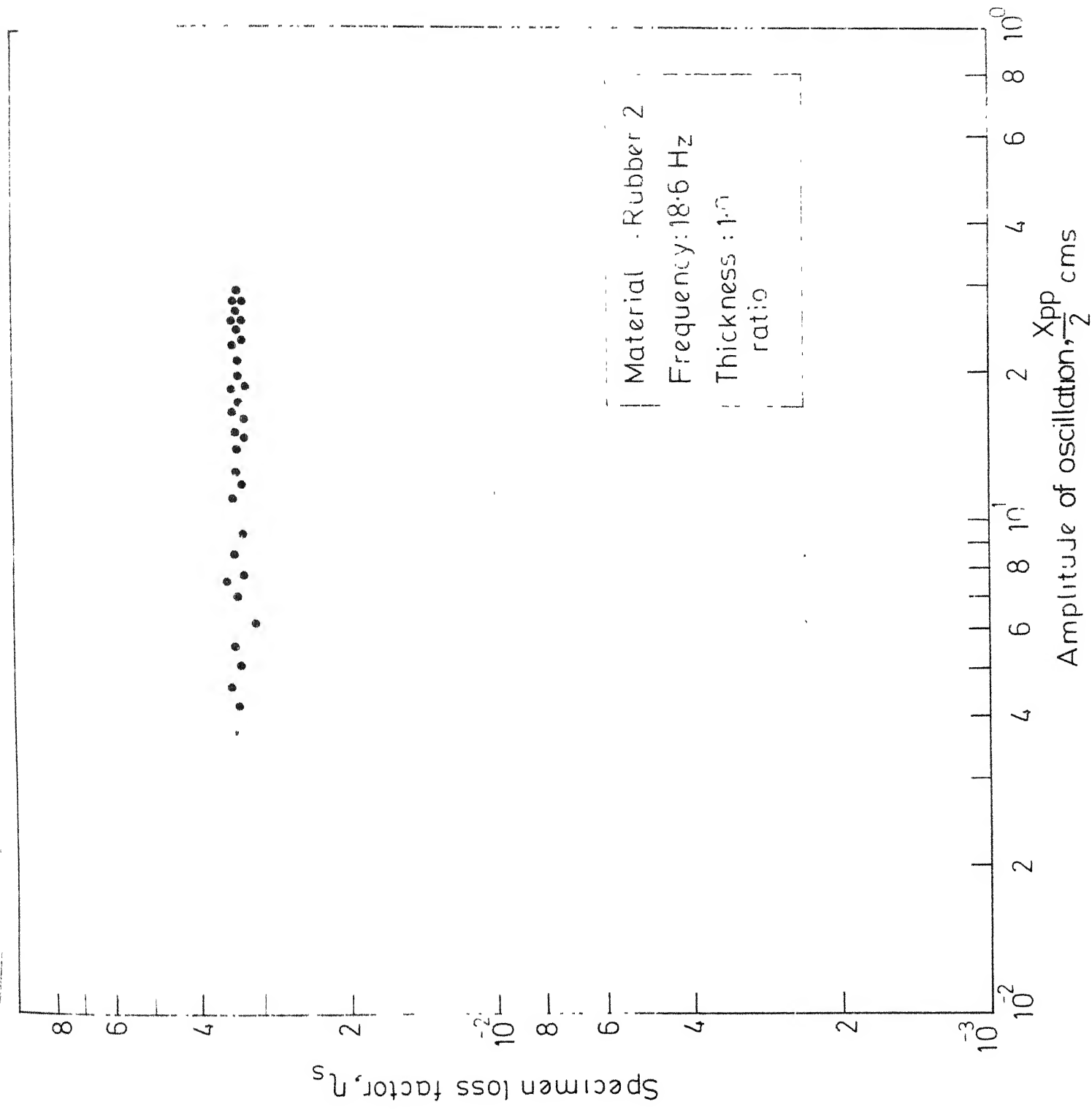


Fig.4.5 Variation of specimen loss factor with amplitude of oscillation

of the order of 0.04. For specimen dimensions used in the present work and a frequency of oscillation 10 Hz, it has been shown in reference [9] that the correction to loss factor for air damping is of the order of 0.001. This being very small compared to the measured specimen loss factor, it was decided to neglect the air damping. Similar checks were also made at higher frequencies. This suggested that for measurements of damping of rubber like materials experiments can be conducted in air without any appreciable error.

#### 4.5 Variation of Loss Factor with Frequency

Figure 4.6 shows the variations of loss factor of all the four materials tested in a range of frequency 10 - 85 Hz. It is clearly seen that the damping capacity of all the materials are very strongly dependent on frequency. The loss factor of all these materials are also found to be very high in this low range of frequency. This is in line with the observation of reference [5] that most of the commercial rubbers have very high damping in a frequency range of 40 - 120 Hz. At very high frequency, of course, the rubber is transformed into a hard glass like substance with very little damping.

For the sample number '1', a small peak is seen around 20 Hz. For 'Durafoam', a rather sharp peak is observed around 60 Hz. For sample number '3', tendency of attaining a maximum value around 80 Hz is also apparent from Figure 4.6.

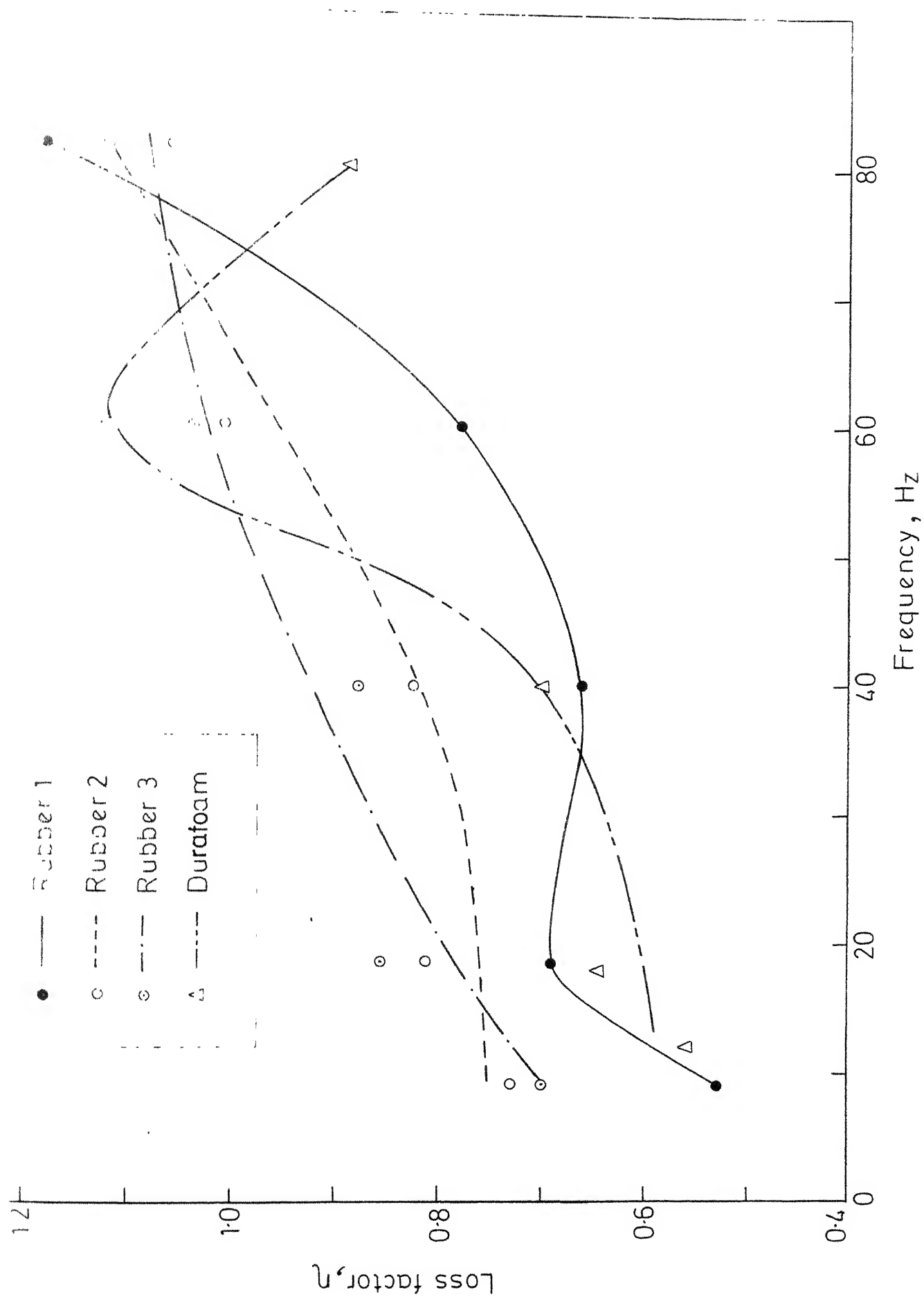


Fig. 4.6 Variation of loss factor with frequency

Comparing the ultimate strength of the rubbers, it can be noted that average damping in the frequency range of the present experiment is more with increasing ultimate strength. However, more of such materials should be tested before making this as a conclusion. It is felt that hardness along with other mechanical properties should be measured to find a confirmed correlation so that an easier to measure static property can be used as an index of damping capacity.

#### 4.6 Variation of Loss Factor with Carbon Content

Figure 4.7 shows the variation of loss factor of all the three rubbers against the carbon content with frequency as a parameter. It can easily be seen that up to 60 Hz, the loss factor increases quite appreciably with increasing <sup>carbon</sup> content up to 35%. At 80 Hz, a slight decrease in damping is seen to occur when the carbon content increases from 15 to 35%. On the whole, 35% carbon content is seen to be most favourable for high damping in the low frequency range up to 80 Hz.

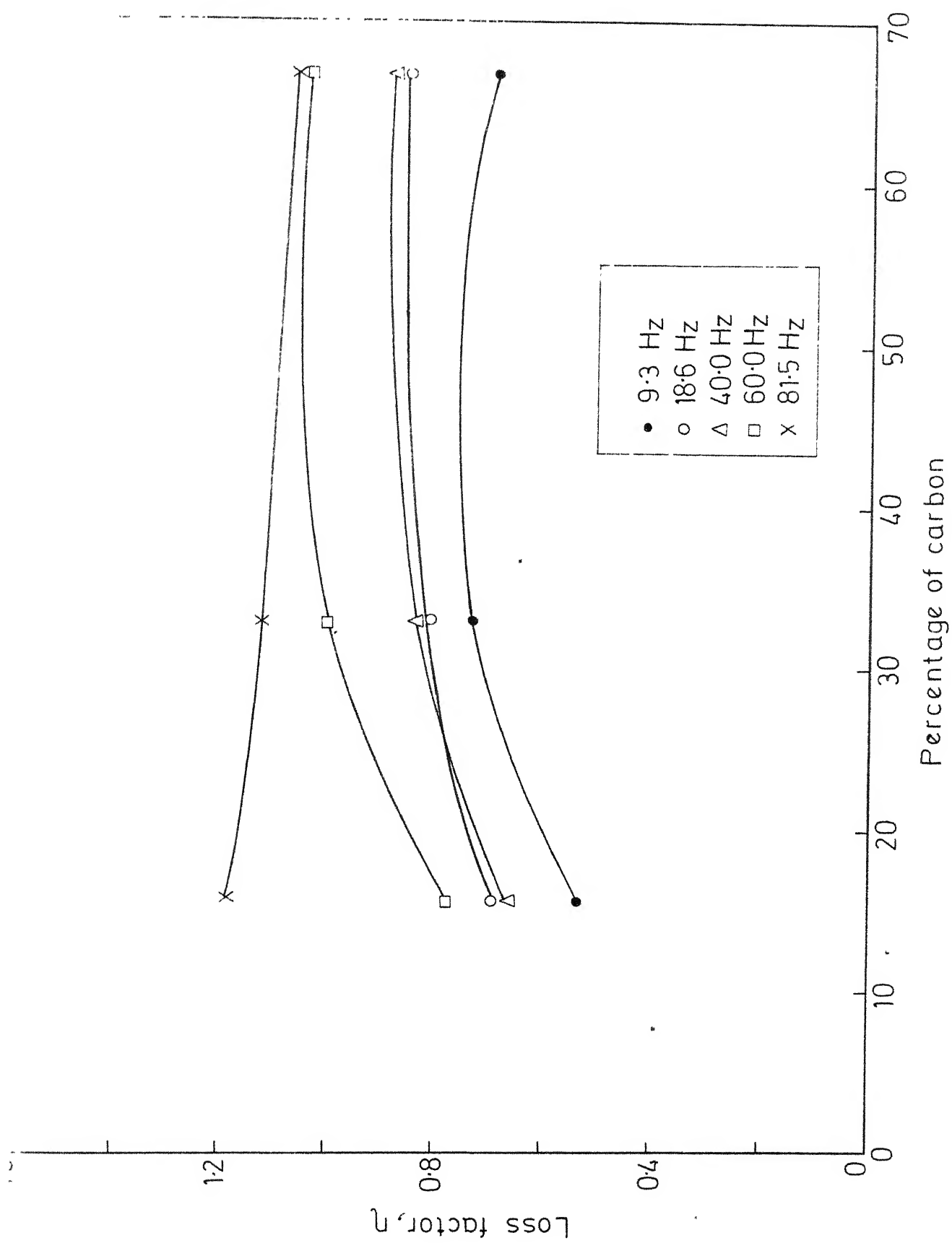


Fig.4.7 Variation of loss factor with carbon percentage

## CHAPTER 5

### CONCLUSIONS

In the light of the results obtained in this investigation, the following conclusions can be drawn.

- i) The damping capacity of very high damping visco-elastic materials can be measured by a forced vibration technique. In this method the energy required to maintain steady state harmonic oscillation of a composite beam specimen is measured.
- ii) For such materials the experiments can be performed in air.
- iii) The damping property of these materials is independent of amplitude but have a strong frequency dependence.
- iv) The beam specimen can be excited only in its first mode due to strong coupling at higher modes.
- v) All the rubbers show high loss factor values in a frequency range of 10 - 85 Hz.
- vi) For rubbers the damping capacity can possibly be related to its tensile strength and carbon content.

## REFERENCES

1. Snowdon, J.C., Vibration and Shock in Damped Mechanical Systems, John Wiley and Sons, Inc., 1968.
2. Nashef, A.D., and Halvorsen, W.G., Design Evaluation of Layered Viscoelastic Damping Treatments, Sound and Vibration, 1978.
3. Kimball, A.L., and Lovel, D.D., Internal Friction in Solids, Physics Review, Vol. 30, p. 948, 1927.
4. Jones, D., and Parin, M.L., Techniques for Measuring Damping Properties of Thin Viscoelastic Layers, Journal of Sound and Vibration, Vol. 24 (2), p. 201, 1972.
5. Marie, R.D., Damping Capacity of Rubber Like Materials Loaded in Compression and Dependence of Their Capacity on Several Parameters, Machine Tool Design Research Proceedings of Tenth International Machine Tool Design Research Conference, University of Manchester, p. 83, 1969.
- 6 - Horio, M., and Onogi, S., Forced Vibration of Reed as a Method of Determining Viscoelasticity, Journal of Applied Physics, Vol. 22, No. 7, p. 977, 1951.
- 7 - Ruzicka, J.E., Structural Damping, Section Five, Pergamon Press, New York, 1960.
- 8 - Ruzicka, J.E., Structural Damping, Section Three, Pergamon Press, New York, 1960.

9. Rakesh Chandra, An Investigation of Damping as a Measure of Damage in Composites, M.Tech. Thesis, Department of Mechanical Engineering, I.I.T. Kampur, 1979.
10. Ingram, G., Methods of Organic Elemental Microanalysis, Chapman and Hall, London, 1962.